Journal of Pharmaceutics & Drug Development
Volume 11 | Issue 1
ISSN: 2348-9782

Research Article Open Access

Unlocking Neurodegeneration: Scaffold-Derived Blockers of MAO-B and AChE Inspired by *Bryophyllum pinnatum*: A Structural Exploration

Ezekiel A Olugbogi[1, 2, *], Emmanuel S Omirin[1, 2], Shola D Omoseeye[1], Blessing T Owolabi[3], Michael A Aderiye[3], Oluwanifemi M Ajayi[3], Victor O Onekhena[3], Daniel A Olatunji[3], Racheal A Adetunji[1, 4], Odunayo B Makanjuola[4], Ayodeji J Ajibare[3], Moshood Folawiyo[3], Olubode O Akintoye[3], and Olaposi I Omotuyi[1, 5]

[1]Molecular Biology and Simulations Center, Ado-Ekiti, Ekiti State, Nigeria
[2]Department of Biochemistry, Adekunle Ajasin University Akungba-Akoko, Ondo State, Nigeria
[3]Department of Physiology, Ekiti State University, Ado Ekiti, Ekiti State, Nigeria
[4]Department of Science Laboratory Technology, Ekiti State University, Ado Ekiti, Ekiti State, Nigeria
[5]College of Pharmacy, Afe Babalola University, Ado-Ekiti, Ekiti State, Nigeria

[*]**Corresponding Author:** Olugbogi Ezekiel Abiola, Molecular Biology and Simulations Center, Ado-Ekiti, Ekiti State, Nigeria, Tel.: +2347032853799, E-mail: olugbogiezekiel@gmail.com

Citation: Ezekiel A Olugbogi, Emmanuel S Omirin, Shola D Omoseeye, Blessing T Owolabi, Michael A Aderiye et al. (2024) Unlocking Neurodegeneration: Scaffold-Derived Blockers of MAO-B and AChE Inspired by Bryophyllum pinnatum: A Structural Exploration, J Pharma Drug Develop 11(1): 103

Received Date: May 01, 2024 **Accepted Date:** June 01, 2024 **Published Date:** June 05, 2024

Abstract

This study evaluates the potential of *Bryophyllum pinnatum* ligands as treatments for Alzheimer's disease (AD) and Parkinson's disease (PD) by targeting acetylcholinesterase (AChE) and monoamine oxidase B (MAO-B), enzymes linked to these neurodegenerative disorders. Utilizing Schrödinger Suite and Maestro 12.8 for computer-aided drug design, ligands from *B. pinnatum* and standard drugs were docked into the active sites of AChE and MAO-B. Further analysis included ADMET screening and MM/GBSA calculations, with pharmacophore modeling to align compounds with reference ligands. The study identified 4 and 6 promising compounds as MAO-B and AChE inhibitors, respectively. Pinoresinol was identified as the most promising candidate, exhibiting optimal binding, favorable blood-brain barrier permeability, and pharmacophoric features similar to those of the standard drug. These findings suggest the neuroprotective capabilities of *B. pinnatum* ligands, recommending further *in vivo* and *in vitro* testing to confirm their therapeutic efficacy.

Keywords: Alzheimer's disease; Parkinson's disease; Bryophyllum pinnatum; AChE and MAO-B inhibitors; Computer-aided drug design

List of Abbreviations: AChE: acetacholinesterase; MAO-B: Mono-amine oxidase B; AD: alzheimers' disease; PD: parkinson's disease; ADMET: adsorbtion distribution metabolism excretion and toxicity; BBB: blood brain barrier; ROV: rule of thumb or Lipinski's rule of five; HBA: hydrogen bond acceptor; HBD: hydrogen bond donor; MM/GBSA: molecular mechanics/generalized born surface area; OPLS4: optimized potentials for liquid simulation-4

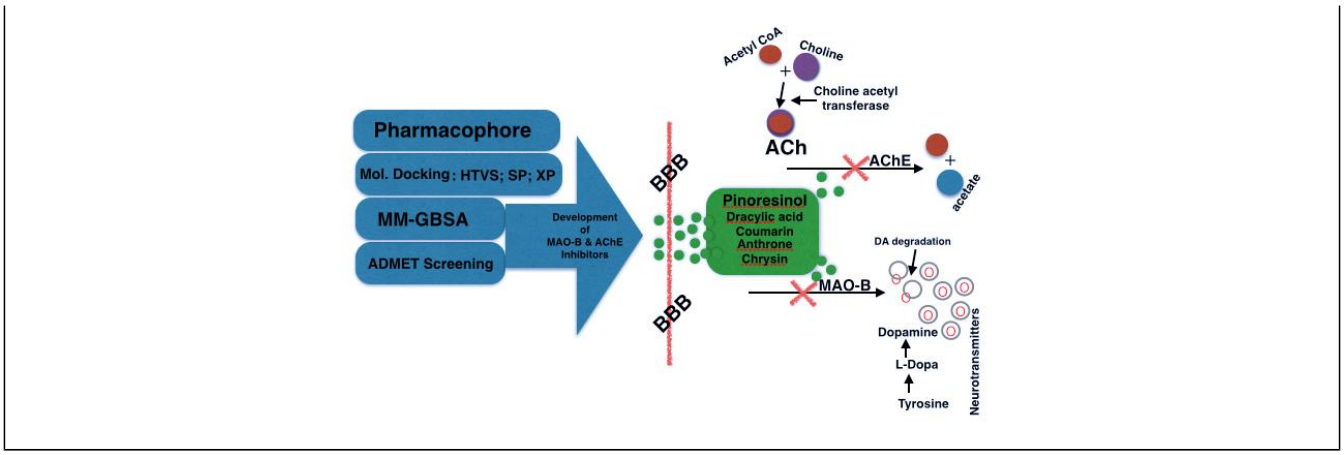

Introduction

Alzheimer's Disease (AD) and Parkinson's Disease (PD) are prevalent neurodegenerative disorders with increasing rate due to longer life span [1]. AD and PD are both progressive and incurable but differ in clinical presentation underlying pathology and affected brain regions. AD is a characterized by progressive memory loss and cognitive decline, it is caused by impairment in the memory and cognition related regions. PD is characterized by motor symptoms such as tremors, bradykinesia (slowness of movement), rigidity, and postural instability [2]. Both AD and PD have overlapping non-motor symptoms and increase in prevalence with age. Current treatments focus on symptoms management rather than a cure.

Acetylcholinesterase (AChE) In Alzheimer's Disease

Acetylcholinesterase (AChE) is an enzyme that breaks down a neurotransmitter called acetylcholine in the brain[3]. In Alzheimer's disease, acetylcholine levels decrease leading to cognitive problems. Cholinesterase inhibitors blocks AChE, temporarily leading to increasing acetylcholine (ACh) and improving memory and cognitive function. AChE's active site consists of two subsites: the anionic site and the esteratic subsite [4]. The esteratic subsite contains the catalytic triad of amino acids involving in hydrolyzing acetylcholine. Acetylcholinesterase inhibitors (AChEIs) are commonly prescribed to address reduced levels of acetylcholine in AD. They inhibit the enzyme AChE, increasing the level and duration of acetylcholine action. AChEIs bind to the perpheral anionic site and prevent the breakdown of acetylcholine. In some cases, such as organophosphate poisoning, this inhibition can be toxic due to the accumulation of acetylcholine in the synapses [5].

The cholinesterase inhibitor drugs which inhibit AChE activity are rivastigmine, galantamine and donepezil. They decrease the breakdown of acetylcholine, maintaining its level [6]. Rivastigmine inhibits AChE and its catalytic activities, while galantamine interacts with the anionic subsite and modulates nicotinic cholinergic receptors. Donepezil binds to the catalytic site of the enzyme, controlling key symptoms of AD. These drugs do not halt disease progression but improve memory and cognitive impairment. They are the main marketed drugs for Alzheimer's treatment.

Monoamine Oxidase-B (MAO-B) In Parkinson's Disease

Monoamine oxidase-B is an enzyme in the body that breaks down several chemicals in the brain, including dopamine [7]. Dopamine is a neurotransmitter responsible for coordinating movement and muscle control. In PD, there is a loss of dopaminergic neurons in the substantia nigra, leading to reduced dopamine levels. MAO-B inhibitors, such as selegiline and rasagiline, are used to address deficit. These inhibitors block MAO-B activity, preventing the breakdown of dopamine and increasing its availability in the brain [8]. By inhibiting MAO-B, these medications help maintain higher dopamine levels, improving neurotransmission and alleviating PD symptoms.

However, excessive inhibition of MAO-B can lead to adverse effects due to excessive dopamine in the brain. Excess dopamine in different brain region can result in psychosis, addiction [9], or movement disorders [2, 10, 11]. Therefore, MAO-B inhibitors must be used in a targeted and controlled manner to prevent excess accumulation of dopamine in the brain, with careful monitoring to maximize therapeutic effects and minimize potential harm.

Bryophyllum pinnatum

Bryophyllum pinnatum, also known as the air plant or leaf of life, is a succulent plant with medicinal potentials [12]. It contains various phytochemicals such as flavonoids, alkaloids, tannins, saponins, sterols, and glycosides. Notable phytochemicals reported in this study from *B. pinnatum* include pinoresinol, octanoic acid, dracylic acid, naicin and coumarin; ferulic acid, chrysin, anthrone and pinoresinol showed to be excellent blockers of AChE (5) and MAO-B (4), respectively. Traditionally, it has been used topically in for wound healing and treating skin conditions. It has been employed to alleviate respiratory symptoms, reduce inflammation, address gastrointestinal issues, and exhibit antioxidant and potential anti-diabetic properties.

Computer-Aided Drug Design

Computer Aided Drug Design (CADD) is a highly effective approach for expediting the drug discovery process and reducing time. It employs various methods, such as database screening and generation of novel scaffolds, to efficiently identify potential drug leads [13]. Molecular docking, a crucial method CADD was used in this study. It investigates how tiny compounds such as phytochemicals interact or behave in a target protein active region [14]. Among the techniques employed are ligand library development and preparation from an online database, target retrieval from a PDB database, receptor grid generation, molecular docking, and ADME-Tox Screening.

Method

Target Preparation and Molecular Docking

Schrödinger Suite software (Maestro 12.8) was used to conduct computer-based drug screening. A total of 121 compounds that have been described with *B. Pinnatum* and the standard drugs were collected from an online database and docked to the active site of MAO-B and AChE to predict compounds with the best inhibitory potential to inhibit MAO-B and AChE action in the treatment of Parkinson's disease and Alzheimer's disease. The 3D structure of MAO-B in complex with rosiglitazone (PDB ID: 4A7A) and AChE in complex with Donepezil (PDB id:7E3H) was downloaded from RCSB protein data bank (https://www.rcsb.org).

The structure was imported and the protein preparation wizard tool in Maestro's Schrodinger Suite was used to prepare the protein. Bond orders were assigned, hydrogens were added, zero-order metal bonds were made, disulfide bonds were created, water molecules were removed, and het states were generated using Epik at pH 7.0 ± 2.0 during the protein production. The protein was refined by optimizing the H-bond assignment and PROPKA pH 7.0 was used. OPLS4 (Optimized potentials for liquid simulation) is a force field used in molecular dynamics and docking simulations. It calculates the energy of molecular systems by considering atom types, bonds, angles, and torsions, enabling realistic modeling of molecular interactions and properties. Water molecules were removed beyond hets 3.0 Å then restrained minimization was done using force field OPLS4 to minimize the protein. The Ramachandran's Plot was then deduced and saved. The prepared ligands were docked following the standard docking protocols which includes High Throughput Virtual Screening (HTVS), Standard Precision (SP), setting the ligand sampling to rigid and Extra Precision (XP) setting the ligand sampling to rigid and flexible.

Receptor Grid Generation

Glide Grid is a component of the Glide software used in molecular docking. It defines the area of a protein where potential ligands will interact, helping in accurate positioning and scoring of these molecules during the docking process [15]. The Receptor Grid

Generation tool was used to create the prepared protein grid on the binding site (Glide Grid) [16]. Selecting the co-crystallized ligand at the active site of 7E3H and 4A7A revealed the binding location. A cubic grid box including all the amino acid residues at the active site was automatically produced. The produced grid's three-dimensional coordinates X, Y, and Z were -43.57 Ao, 37.99 Ao& -30.21 Ao and 50.73 Ao, 157.29 Ao& 29.10 Ao for AChE and MAO-B respectively.

Ligand Preparation

The selected 121 ligands used for this study were gotten from Pubchem (https://pubchem.ncbi.nlm.nih.gov). The compound (ligands) was downloaded in SDF format. The ligands were the imported and prepared using Ligprep tool Maestro 12.8 using OPLS4 force field and neutralizing the ionization and generation of at most 1 stereoisomer per ligand.

ADMET Screening

The pharmacokinetic profile, drug-likeness, and toxicity study of the ligands were determined using the SwissADME (http://www.swissadme.ch), Pro-Tox II online servers (https://tox-new.charite.de/protox_II), and ADMETsar was then used to carry out the ADMET properties prediction [17]. The ADMET properties of a compound shows the absorption, distribution, metabolism, excretion, and toxicity in and through the human body [18]. MW (Molecular weight), HBA (number of hydrogen bond acceptors), HBD (number of hydrogen bond donors), ILogP, Logkp and TPSA(Topological polar surface area) were calculated on the basis of Lipinski rule of five [19].

MM/GBSA

The Molecular Mechanics/Generalized Born Surface Area (MM/GBSA) was used to determine the docked protein–ligand complex binding free energy [20]. To complete this project, we selected the protein-ligand complex and VGSB salvation model and OPLS4 force field was used.

Receptor Ligand Complex Pharmacophore Modelling

Pharmacophore was used to identify the compounds that match the pharmacophoric features of the reference ligands of the target receptor. The crystal structure of the protein AChE (PDB ID:7E3H) and MAO B (PDB ID:4A7A) in complex with their reference ligands (Donepezil for AChE and Rosiglitazone for MAO-B) was used. Pharmacophore hypothesis tool in Schrodinger maestro 12.8 was used to develop pharmacophore and identify the pharmacophoric features exhibited by the reference ligand, and it revealed the features; Hydrogen Bond Acceptor (HBA), Hydrogen Bond Donor (HBD), Aromatic ring and hydrophobic region. The selected compounds were subjected to pharmacophore feature matching screening using phase ligand screening module, (2/3 matches for 4A7A) and (4/5 matches for 7E3H). After the screening, all hit compound were subjected to molecular docking and their fitness score were also gotten.

Results and Discussion

Neurodegenerative disorders like Alzheimer's disease (AD) and Parkinson's disease (PD) result in the gradual deterioration of specific groups of neurons. Current therapeutic strategies focus on symptom management rather than disease modification [21]. AD is characterized by progressive memory disorder, while PD primarily manifests motor symptoms due to the loss of dopaminergic neurons [22]. Pharmacological interventions such as acetylcholinesterase inhibitors (AChEI) for AD and MAO-B inhibitors for PD aim to alleviate symptoms by balancing neurotransmitters [23, 24]. *B. pinnatum* shows potential as a source of natural inhibitors against AChE and MAO-B, with promising compounds like Pinoresinol and ferulic acid. These findings suggest the plant's neuroprotective properties and its potential for developing novel therapeutics for AD and PD. In this research, we assessed via *in-silico* study the ligands of *B. pinnatum* with the highest overall potential to be a medication based on its inhibitory ability, blood brain barrier permeability, and toxicity but not limited to against both MAO-B and AChE target proteins for PD and AD. This

was thoroughly explored and compared with the standard drugs for MAO-B and AChE inhibition respectively.

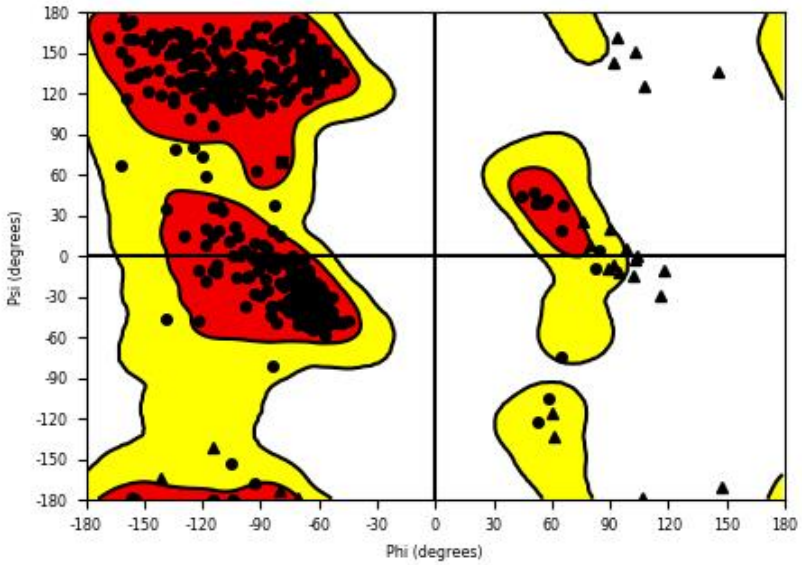

Figure 1i: Ramachandran Plot of the crystal structure of MAO-B

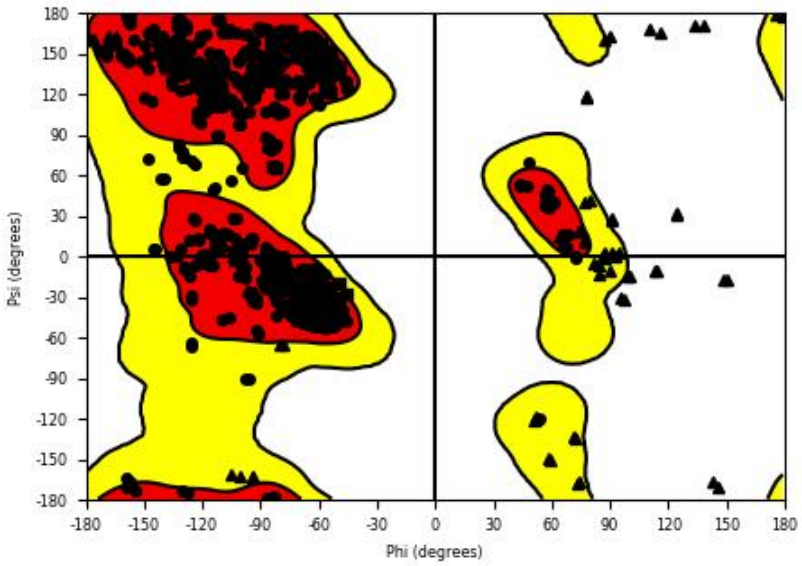

Figure 1ii: Ramachandran Plot of the crystal structure of AChE

The Ramachandran plot provides a statistical distribution of Phi and Psi dihedral angles for an unidentified amino acid (X) within an Ala-X-Ala tripeptide. It helps predict the secondary structure of a protein by analyzing the Psi and Phi values. Figure (1i) and (1ii) show the Ramachandran plots of the crystal structures of MAO-B (4A7A) and AChE (7E3H), respectively, which aid in understanding the secondary structure of these proteins.

Table 1i: Docking and MM/GBSA scores for the top 20 phytochemicals from B. pinnatum interacting with the crystal structure of MAO-B

Compound name	Docking Score (kcal/mol)	*MM/GBSA* (kcal/mol)
Quercetin	-11.582	-24.93
Taxifolin	-11.446	-40.38
Betaxanthin	-11.322	-48.79
Catechin	-10.557	-38.26
Pinoresinol	-10.281	-35.82
Myricetol	-10.221	-38.33
Chlorogenic Acid	-9.549	-36.92
Hesperetin	-9.508	-26.53
Ellagic acid	-9.415	-34.33
Chrysin	-9.214	-18.54
Artocarpanone	-8.997	-25.30
Morin	-8.974	-32.76
Inositol	-8.773	-23.84
Anthrone	-8.748	-33.50
Peonidin	-8.692	-60.74
Kaempferol	-8.578	-36.30
Superoxide dismutase	-8.388	-23.87
Xylose	-8.179	-42.93
Fructose	-8.127	-41.59
Caffeic acid	-8.061	-37.77

Table 1ii: Docking and MM/GBSA scores for the top 20 phytochemicals from *B. pinnatum* interacting with the crystal structure of AChE

Compound name	Docking Score (kcal/mol)	*MM/GBSA* (kcal/mol)
Myricetol	-13.609	-50.59
Taxifolin	-13.234	-56.25
Catechin	-12.827	-54.04
Kaempferitrin	-12.826	-40.4
Thiamine	-11.762	-63.00
Isorhamnetin	-11.550	-46.64
Betuletol	-11.435	-47.48
Artocarpanone	-11.405	-33.13
Morin	-11.269	-22.74
Kaempferol	-11.257	-47.52

Hesperetin	-11.126	-32.32
Betaxanthin	-11.041	-20.89
Chlorogenic acid	-10.898	-29.61
Betacyanin	-10.853	-63.96
Pinoresinol	-10.767	-36.90
Ellagic acid	-10.726	-67.11
Methyl brevifolincarboxylate	-10.669	-57.13
Peonidin	-10.651	-78.44
Artoflavanone	-10.612	-36.27
Betalains	-10.542	-47.36

Table 2i: Docking and MM/GBSA scores for selected phytochemicals from *B. pinnatum* and conventional monoamine oxidase-B inhibitors, assessed based on their blood-brain barrier permeability and interaction with MAO-B

Compound name	**Docking Score (Kcal/mol)**	***MM/GBSA* (Kcal/mol)**
Chrysin	-9.214	-18.54
Pinoresinol	-10.281	-35.82
Anthrone	-8.748	-33.50
Ferulic acid	-7.939	-35.93
Selegiline	-7.416	-24.89
Rasagiline	-7.161	-21.48

Table 2ii: Docking and MM/GBSA scores for selected phytochemicals from *B. pinnatum* and standard acetylcholinesterase inhibitors, assessed based on their blood-brain barrier permeability and interaction with AChE

Compound name	**Docking Score (Kcal/mol)**	***MM/GBSA* (Kcal/mol)**
Dracylic acid	-7.490	-28.59
Octanoic acid	-6.406	-31.47
Niacin	-7.102	-26.11
Pinoresinol	-10.767	-36.90
Coumarin	-7.696	-40.03
Donepezil	-11.186	-54.30
Galantamine	-7.002	-35.25
Rivastigmine	-6.104	-29.57

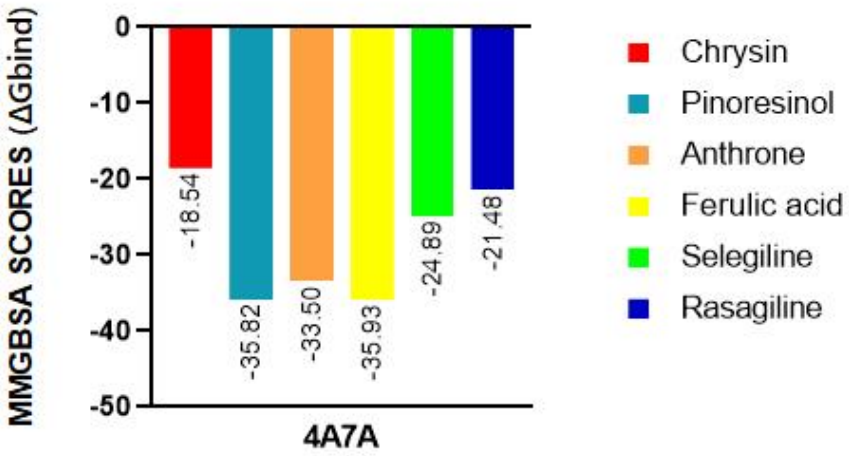

Figure 2i: Graphical representation of the *MM/GBSA* scores of the selected phytochemicals of *B. pinnatum* and the standard MAO-B inhibitors

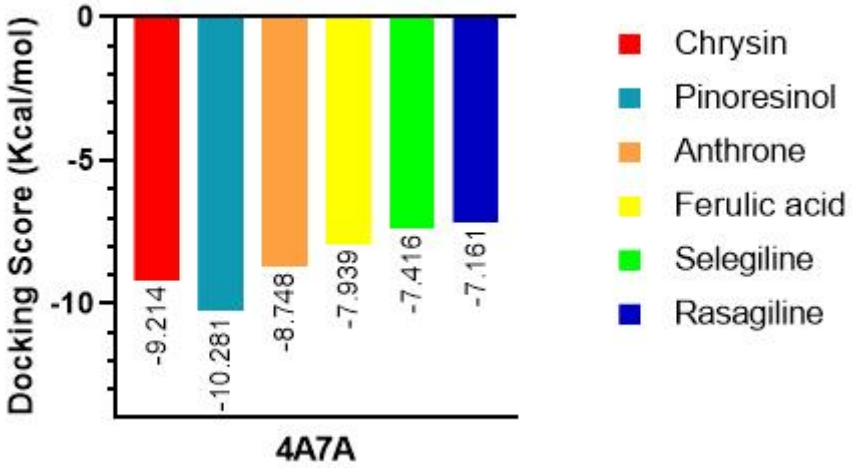

Figure 2ii: Graphical representation of the docking scores of the selected phytochemicals of *B. pinnatum* and the standard MAO-B inhibitors

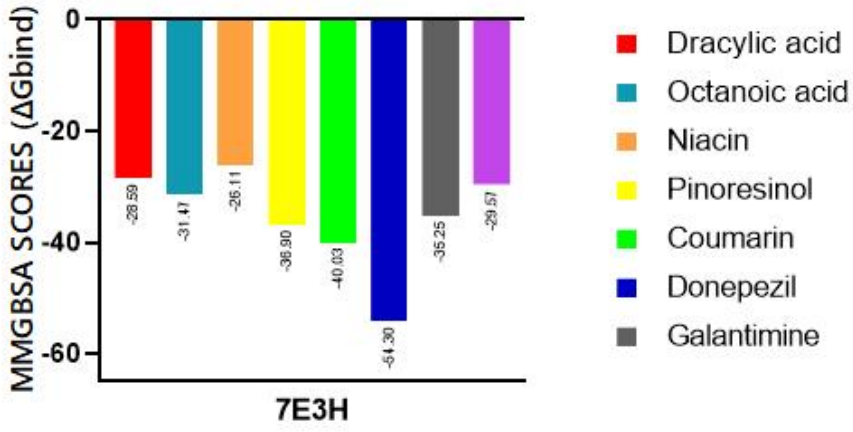

Figure 3i: Graphical representation of the *MM/GBSA* scores of the selected phytochemicals of *B. pinnatum* and the standard AChE inhibitors

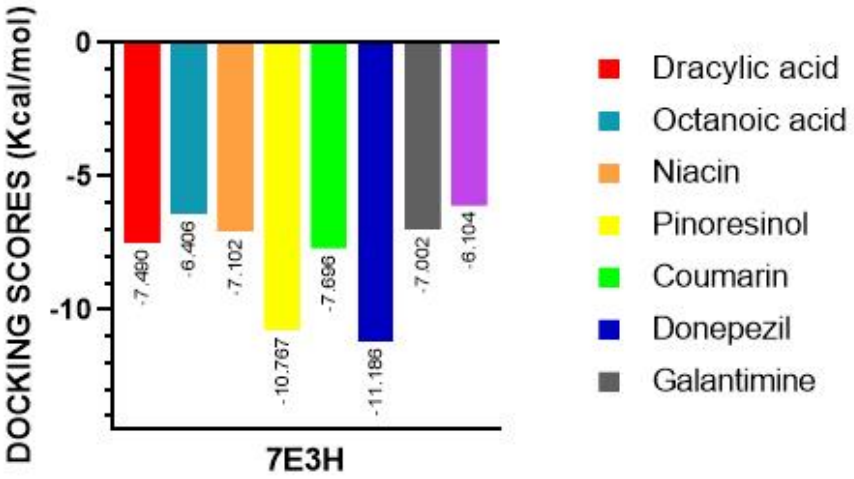

Figure 3ii: Graphical representation of the docking scores of the selected phytochemicals of *B. pinnatum* and the standard AChE inhibitors

Table 1(i) and (ii) present the docking scores and *MM/GBSA* values of the top scoring 20 ligands of *B. pinnatum* screened against MAO-B and AChE, respectively. Table 2(i) and (ii) include the selected ligands and standard drugs, that can penetrate the Blood--Brain Barrier (BBB) for neurologically related diseases. Chrysin, pinoresinol, anthrone, and ferulic acid exhibit strong binding energy with MAO-B, while dracylic acid, octanoic acid, niacin, pinoresinol, and coumarin show strong binding energy with AChE. These ligands outperformed synthetic inhibitors in terms of docking scores and binding free energy as demonstrated in table 2(i) and (ii).

The selected ligands, particularly pinoresinol, show promising potential as inhibitors for MAO-B and AChE. It can penetrate the Blood-Brain Barrier and have superior docking scores compared to the standard drugs. Furtherly, the compound demonstrates a high binding affinity for MAO-B and the second best for AChE, suggesting its potential as a novel and effective treatment for these neurological diseases. In the context of Molecular Mechanics/Generalized Born Surface Area (MM/GBSA), a more negative value for the binding affinity indicates a stronger binding between a ligand and a target [25]. The ligands exhibit stronger binding affinity, as indicated by more negative MM/GBSA scores, compared to the standard drugs. Figures (2i), (2ii), (3i), and (3ii) provide graphical representations of the docking scores and MM/GBSA values for the ligands and standard inhibitors.

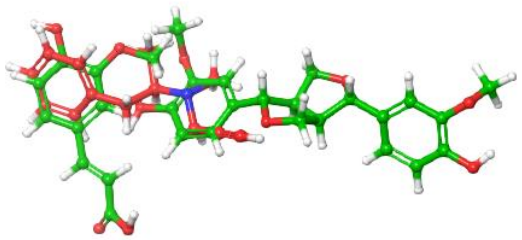

Figure 4i: Superimposed ball-and-stick view of the native (red) and docked (green) pose of the reference ligand (Selegiline) in the active site of MAO-B

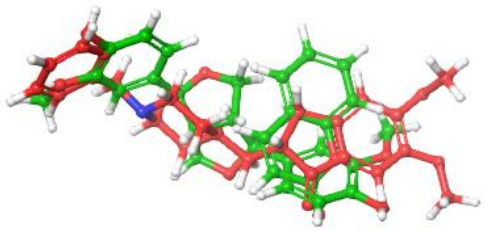

Figure 4ii. Superimposed ball-and-stick view of the native (red) and docked (green) pose of the reference ligand (Donepezil) in the active site of AChE

The Ball and stick representation of the superimposed *B. pinnatum* ligands and the MAO-B and AChE inhibitors further showed the structural similarities and functional groups as confirmed by the pharmacophore screening enabling their binding affinity (Figure 4i and 4ii respectively).

Table 3i: Obtained fitness scores of the phytochemicals of *B. pinnatum* and the standard MAO-B inhibitors

Compound Name (4A7A)	Fitness Score
Chrysin	0.407
Pinoresinol	1.848
Anthrone	0.412
Ferulic acid	0.423
Selegiline	0.421

Table 3ii: Obtained fitness scores of the phytochemicals of *B. pinnatum* and the standard AChE inhibitors

Compound Name (7E3H)	Fitness Score
Octanoic acid	0.117
Pinoresinol	1.563
Coumarin	0.182
Donepezil	2.53
Galantamine	1.423
Rivastigmine	1.492

The fitness score of a drug measures its effectiveness and suitability for treating a specific condition [28]. In the case of selected phytochemical constituents from *B. pinnatum*, Table 3i indicates that these ligands have higher fitness scores compared to standard MAO-B inhibitors. Ligands like ferulic acid and pinoresinol even have higher fitness scores than the standard drugs selegiline and rasagiline. Similarly, Table 3ii shows that the selected ligands have high fitness scores, particularly pinoresinol, compared to standard AChE inhibitors. These factors suggest the potential of these phytochemicals as excellent blockers of MAO-B and AChE.

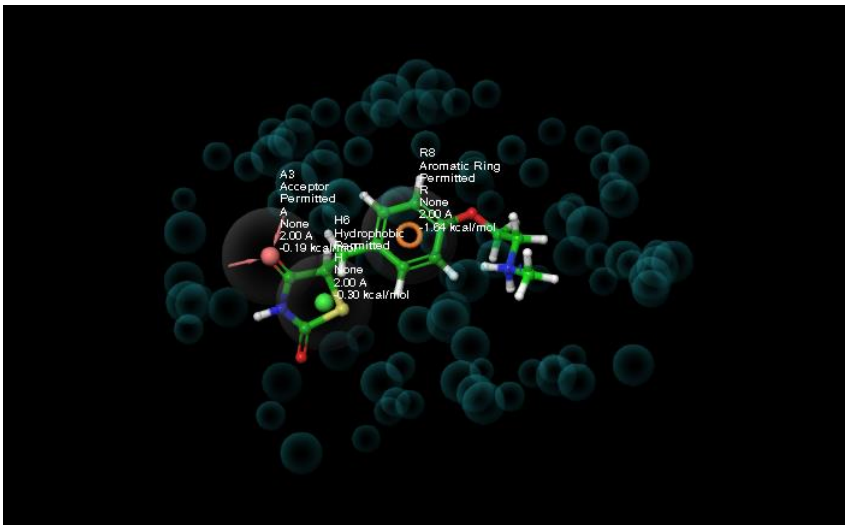

Figure 5i: The pharmacophore features of the reference ligand and the crystal structure of Monoamine oxidase B (4A7A)

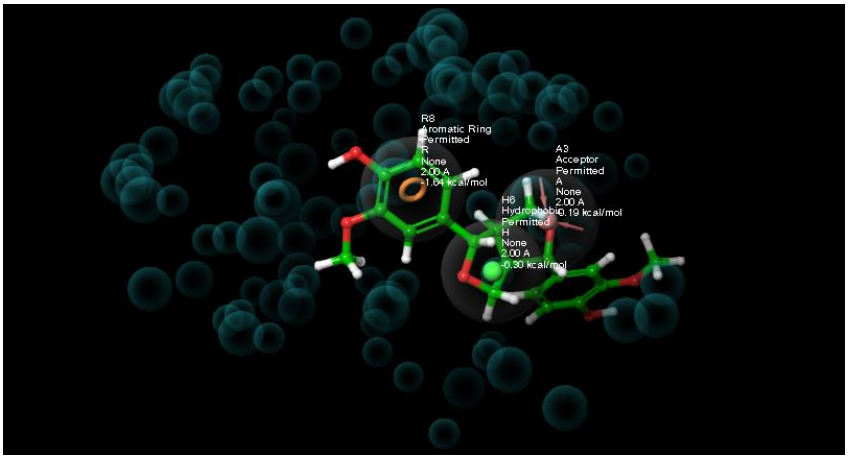

Figure 5ii: The pharmacophore features of *B. pinnatum*'s ligand*:* pinoresinol and the crystal structure of Monoamine oxidase-B (4A7A)

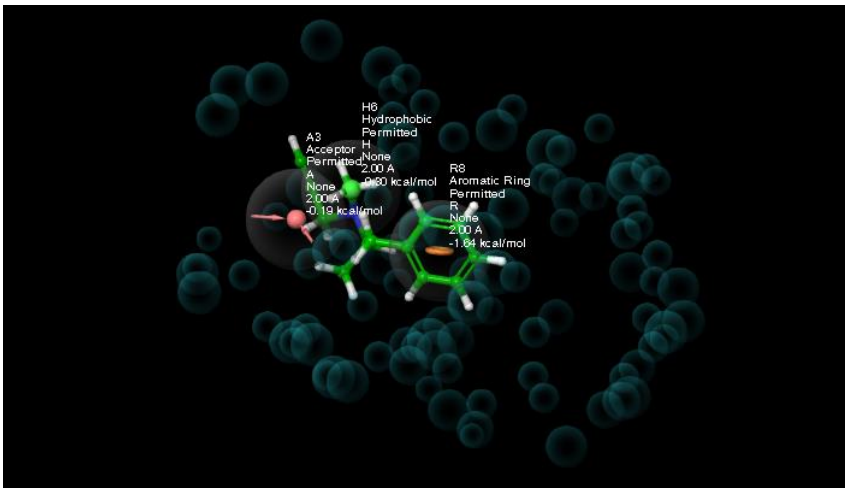

Figure 5iii: The pharmacophore features of a standard drug, selegiline and the crystal structure of Monoamine oxidase-B (4A7A)

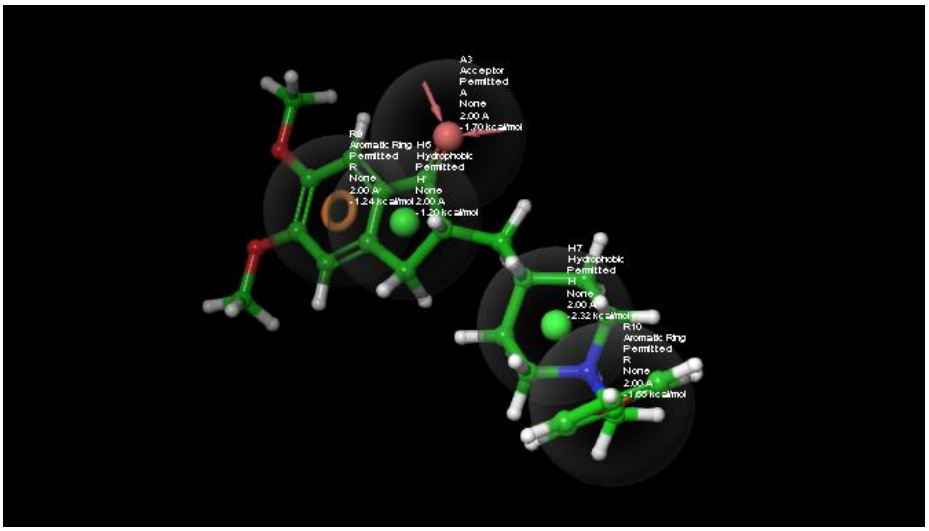

Figure 6i: The pharmacophore features of the reference ligand and the crystal structure of Acetylcholinesterase (AChE).

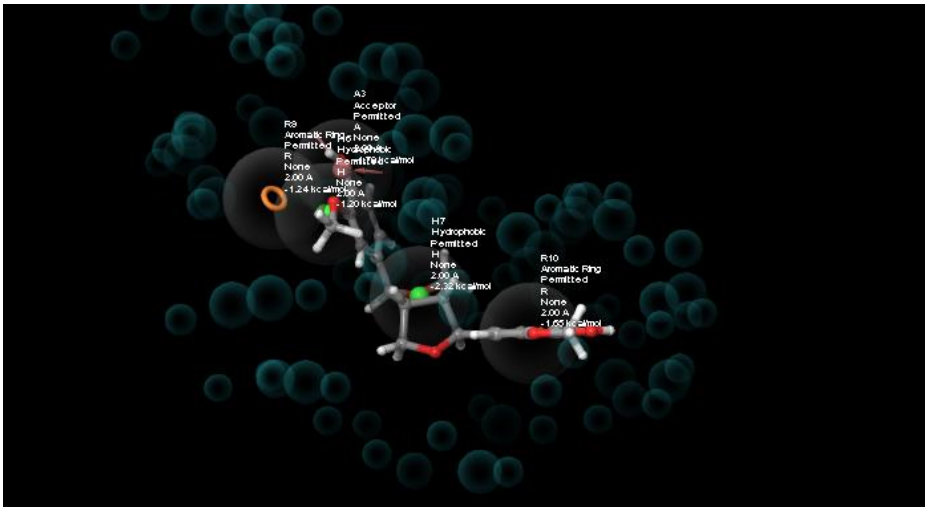

Figure 6ii: The pharmacophore features of *B. pinnatum*'s ligand: pinoresinol and the crystal structure of Acetylcholinesterase (7E3H)

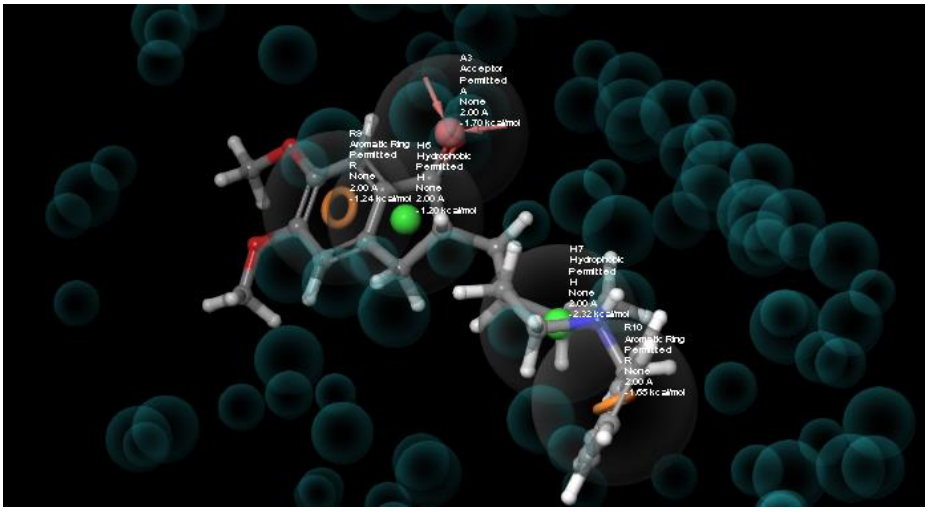

Figure 6iii: The pharmacophore features of the standard drug (donepezil) and the crystal structure of Acetylcholinesterase (7E3H)

Another computational parameter evaluated was pharmacophores, it is an essential molecular feature responsible for a compound's biological activity and interaction with target receptors or enzymes [26, 27]. The reference ligands of MAO-B and AChE crystal structures have specific pharmacophore features such as aromatic rings, hydrophobic regions, and hydrogen bond acceptors as shown in Fig 5i and 6i respectively. Pinoresinol, a phytochemical constituent of *B. pinnatum*, shares common pharmacophore features with the reference ligands of both MAO-B and AChE indicating its potential for binding and activity similar to these reference ligands (Fig 5ii, 5iii, 6ii and 6iii).

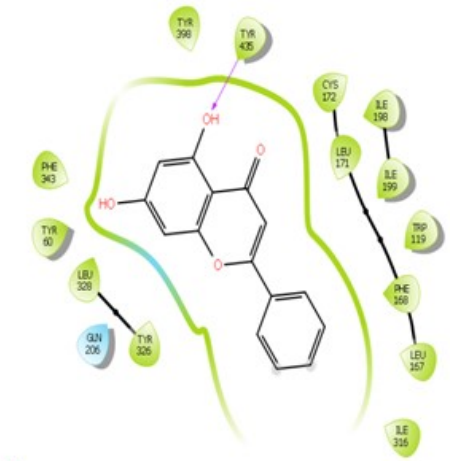

A

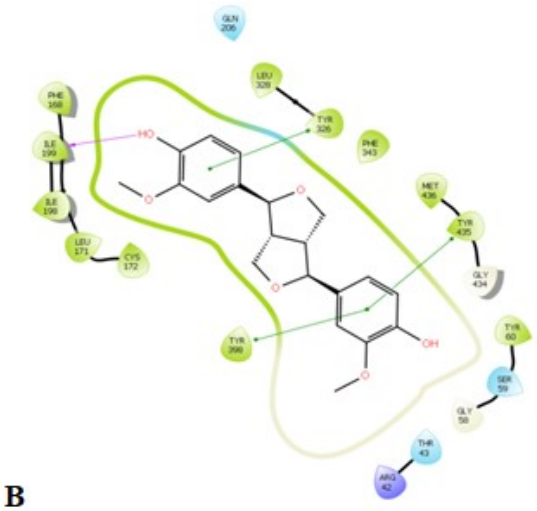

B

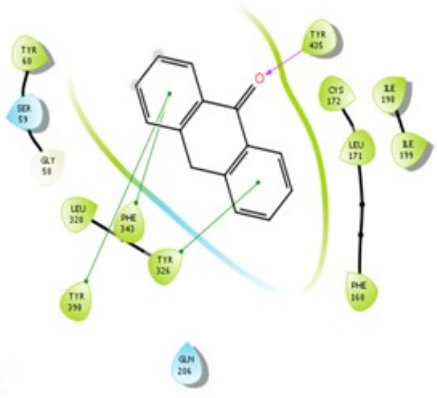

C

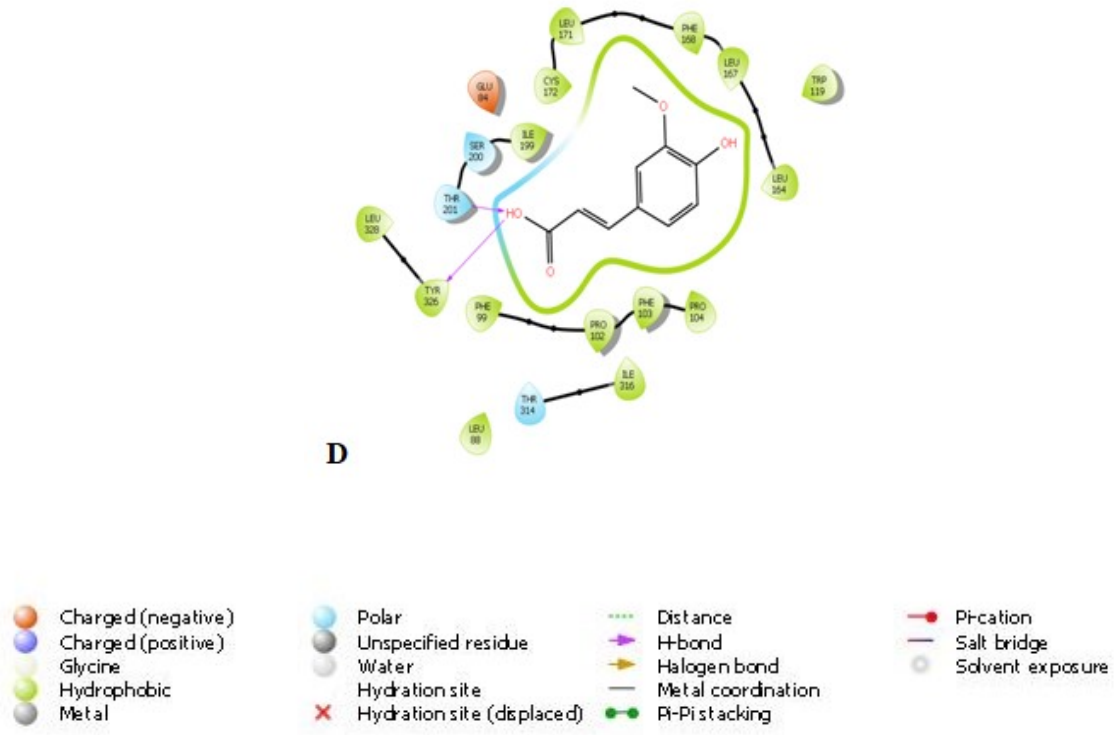

Figure 7i: 2D-Molecular interactions of amino-acid residues of the crystal structure of MAO-B (4A7A) with the photo-chemical constituents of B. pinnatum: A Chrysin B Pinoresinol C Anthrone D Ferulic acid

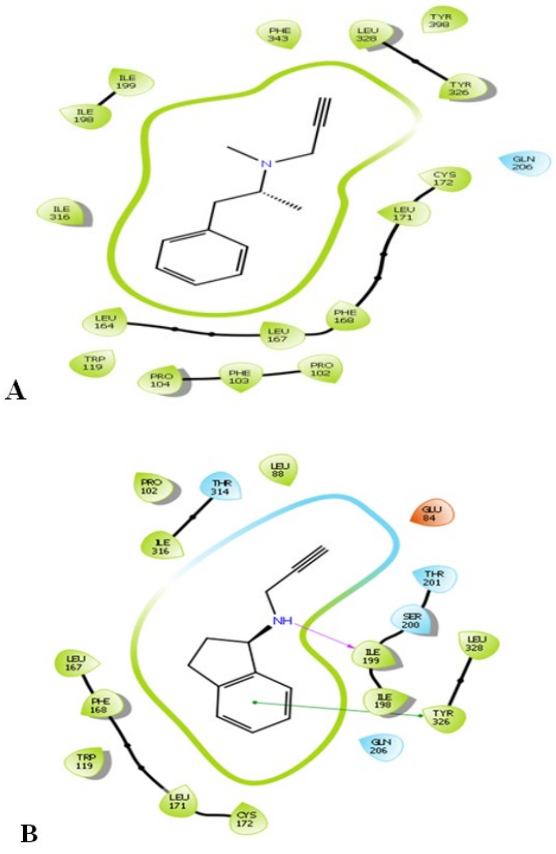

Figure 7ii: 2D-Molecular interactions of amino-acid residues of the crystal structure of MAO-B (4A7A) with MAO-B inhibitors: A Selegiline B Rasagiline

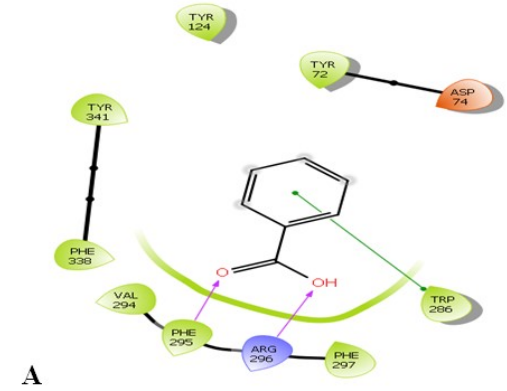

A

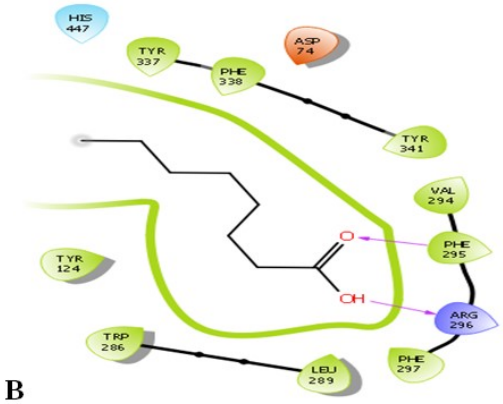

B

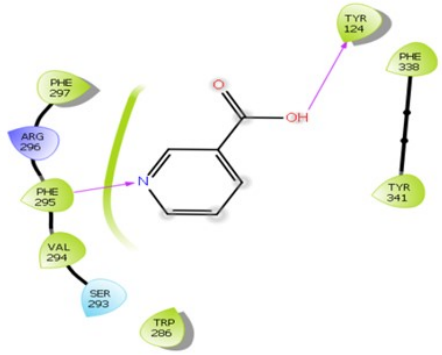

C

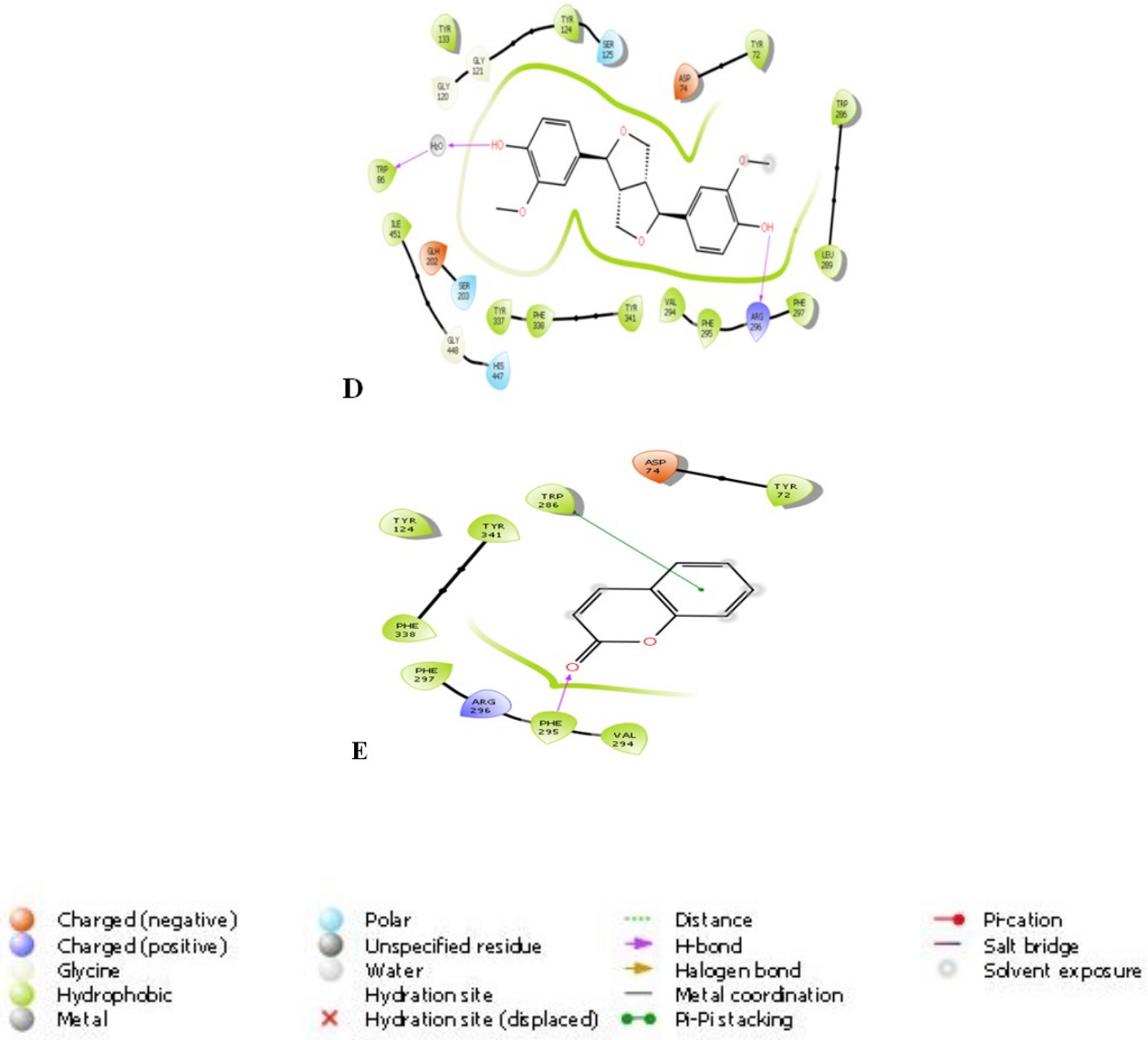

Figure 8i: 2D-Molecular interactions of amino-acid residues of the crystal structure of AChE (7E3H) with the photochemical constituents of B. pinnatum: A Dracylic acid B Octanoic acid C Niacin D Pinoresinol E Coumarin

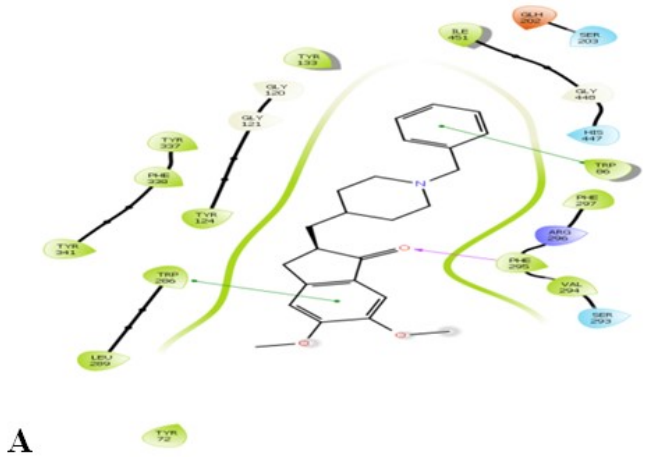

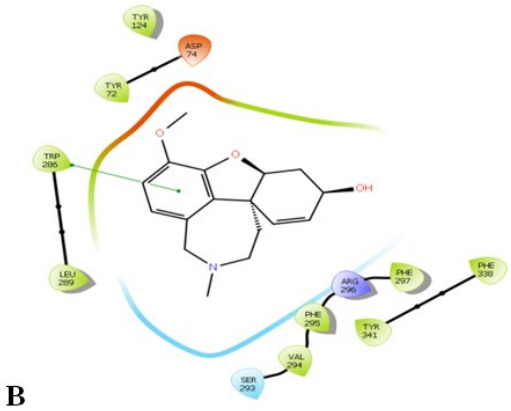

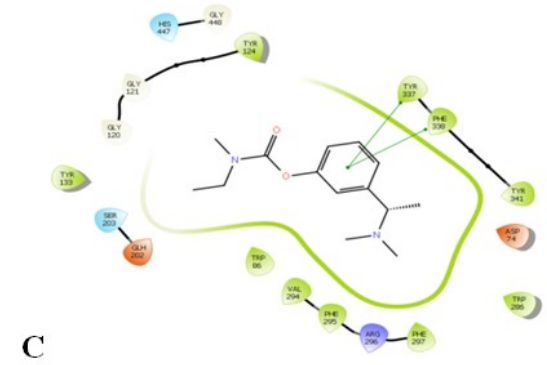

Figure 8ii: 2D-Molecular interactions of amino-acid residues of the crystal structure of AChE (7E3H) with AChE inhibitors: A Donepezil B Galantamine C Rivastigmine

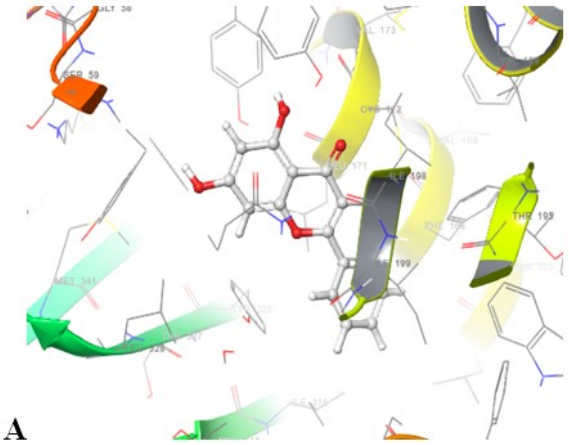

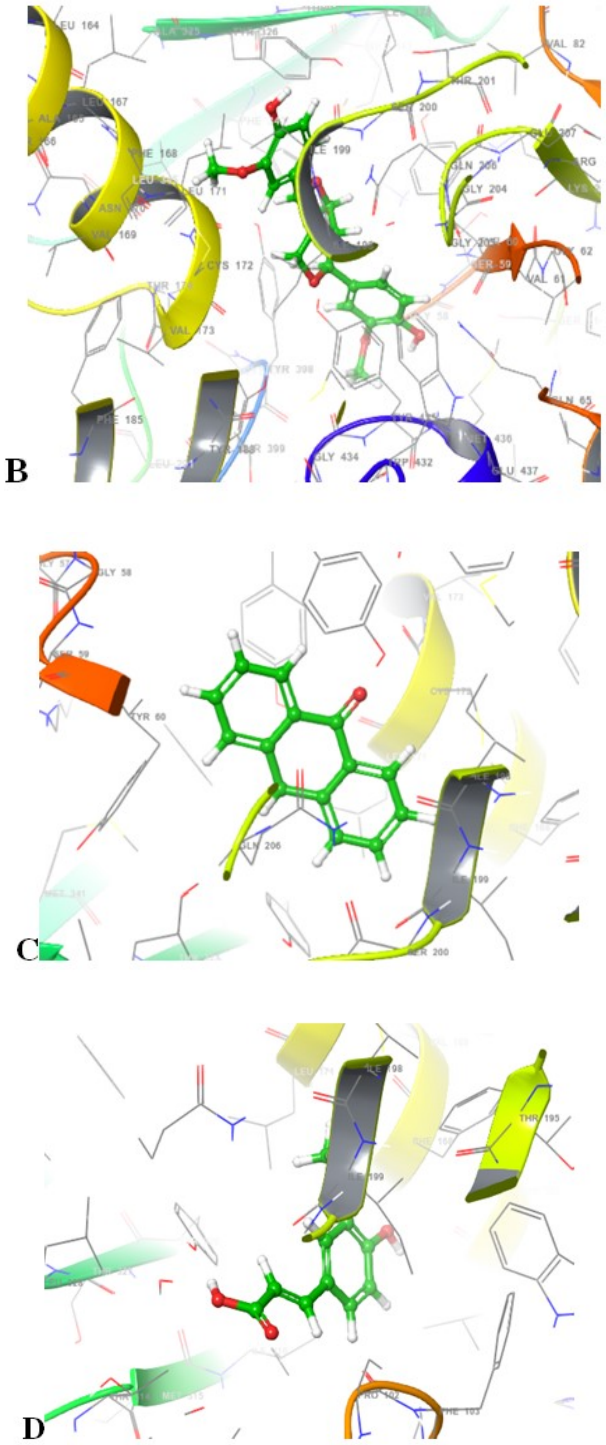

Figure 9i: 3D-Molecular interactions of amino-acid residues of the crystal structure of Monoamine oxidase-B (4A7A) with the ligands of *B. pinnatum*: A Chrysin B Pinoresinol C Anthrone D Ferulic acid

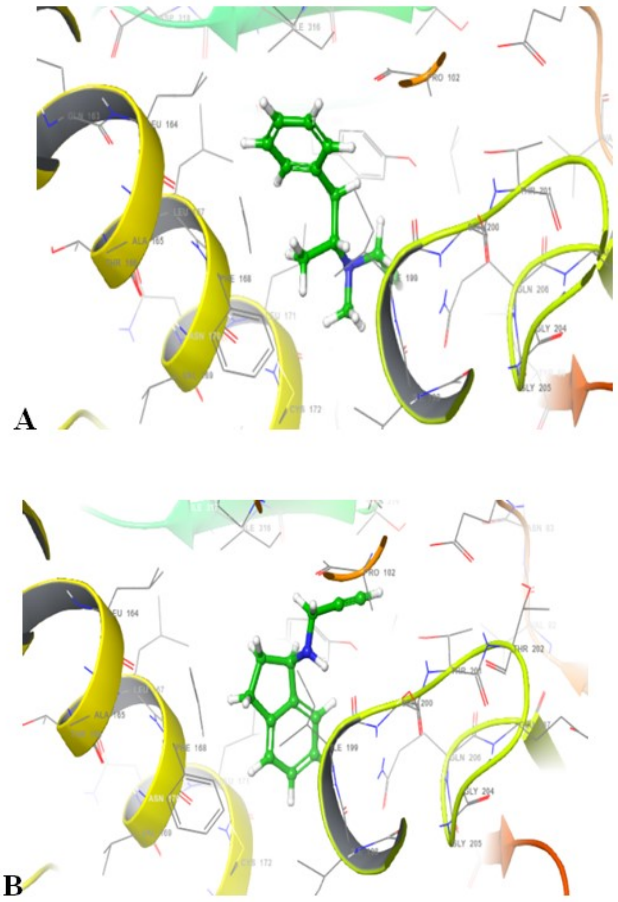

Figure 9ii: 3D-Molecular interactions of amino-acid residues of the crystal structure of MAO-B (4A7A) with MAO-B inhibitors: A Selegiline, B Rasagiline

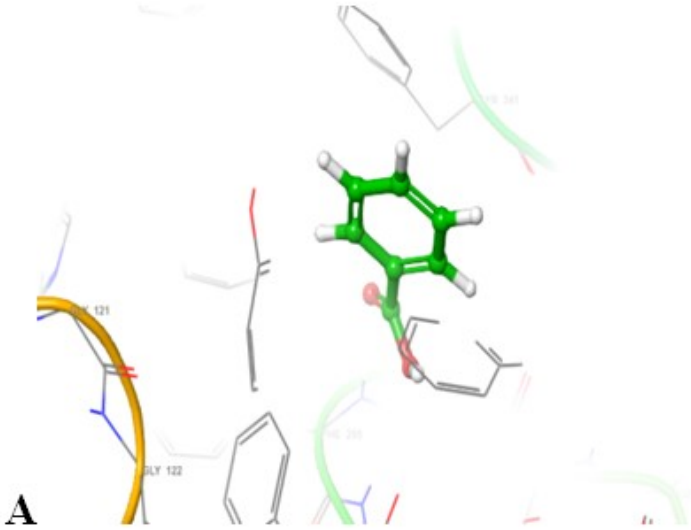

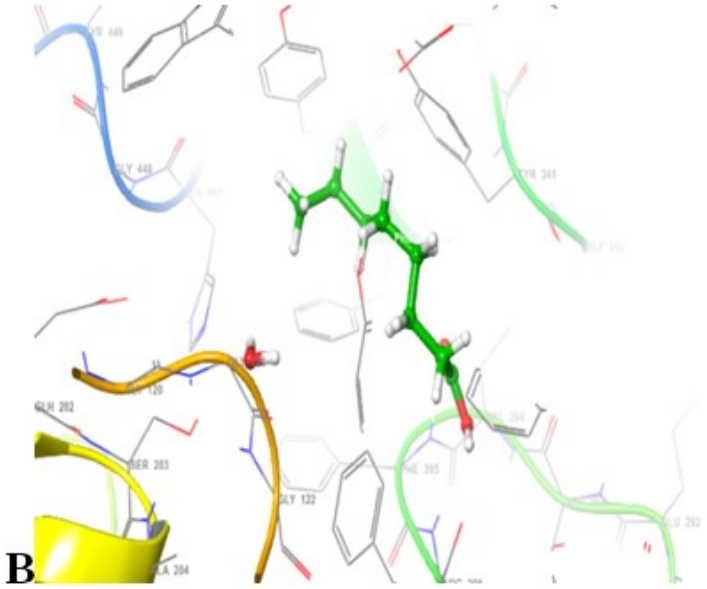
B

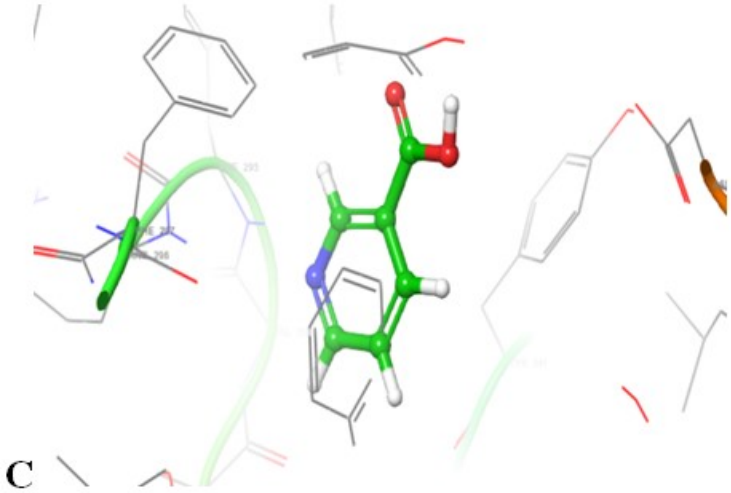
C

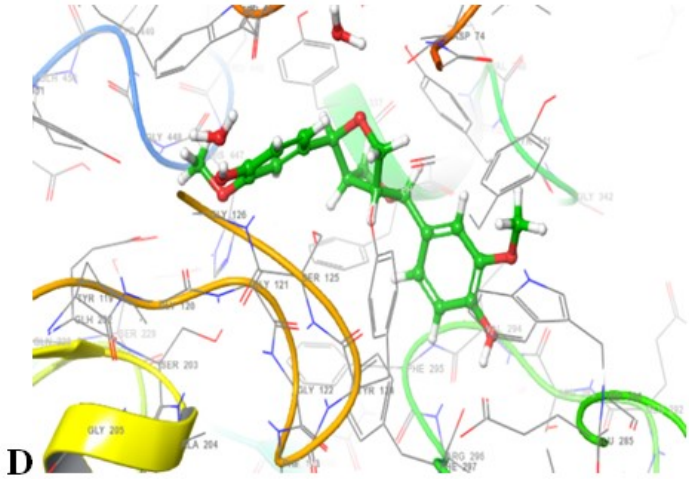
D

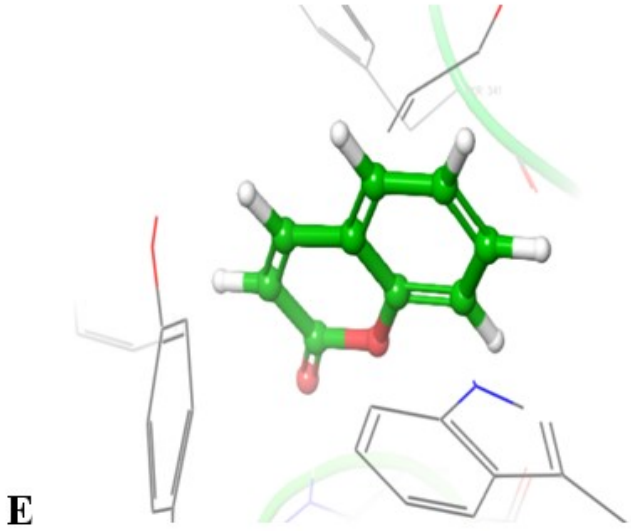

Figure 10i: 3D-Molecular interactions of amino-acid residues of the crystal structure of AChE (7E3H) with the ligands of *B. pinnatum*: A Dracylic acid B Octanoic acid C Niacin D Pinoresinol E Coumarin

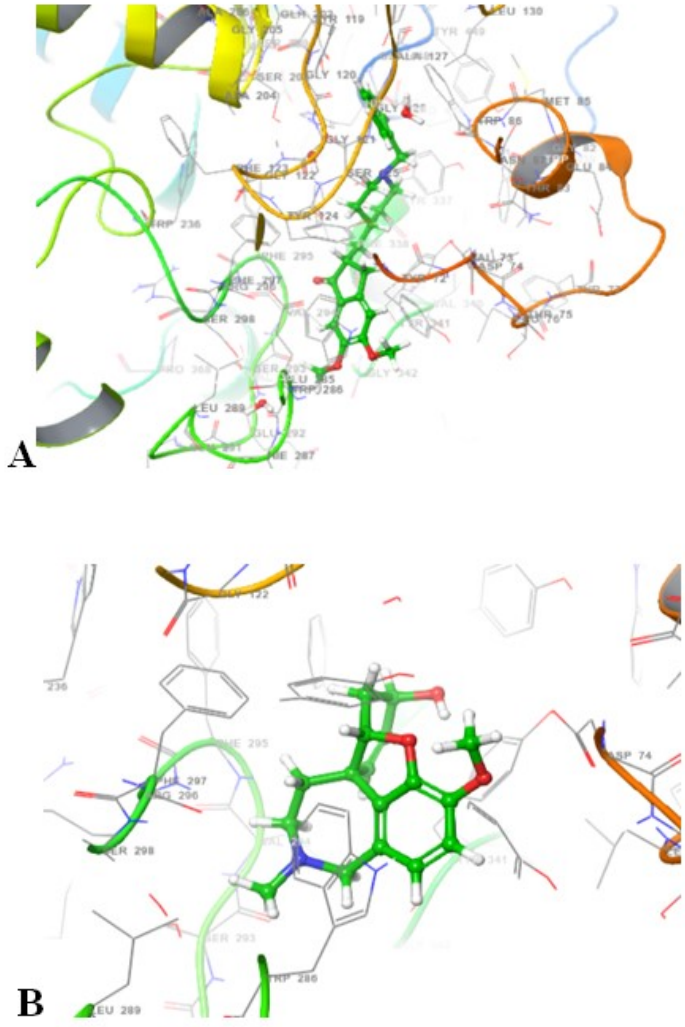

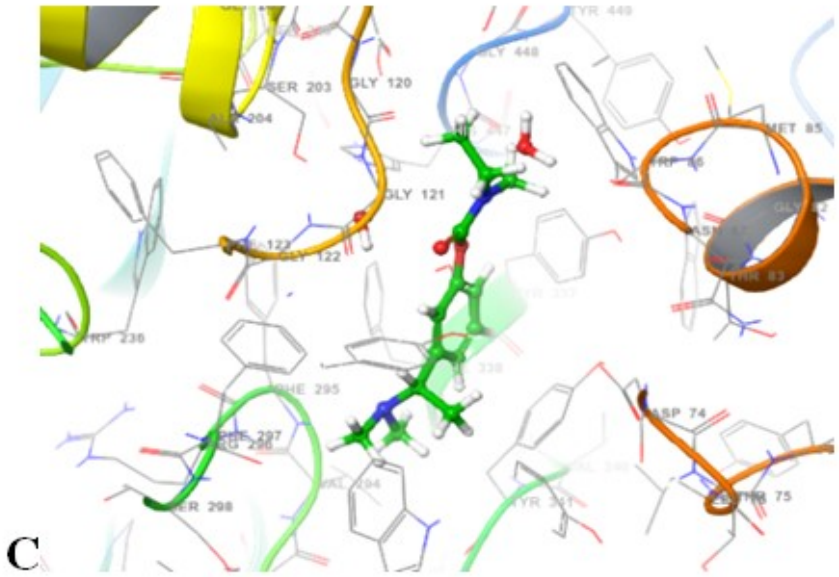

Figure 10ii: 3D-Molecular interactions of amino-acid residues of the crystal structure of Acetylcholinesterase (7E3H) with AChE inhibitors: A Donepezil, B Galantimine, C Rivastigmine

Table 4i: Hydrogen Bonds, Hydrophobic interactions, and other contacts of the ligands of *B. pinnatum* and the standard MAO-B inhibitors with MAO-B

Compound Name	Docking Score (kcal/mol)	H-BOND	Hydrophobic interacting amino acids	Other Interactions
Chrysin	-9.214	TYR 435	TYR 398, TYR 435, CYS 172, LEU 171, PHE 168, LEU 167, ILE 316, ILE 198, ILE 199, TRP 119, PHE 343, TYR 60, LEU 328, TYR 326	None
Pinoresinol	-10.281	ILE 199	TYR 398, CYS 172, LEU 171, ILE 198, ILE 199, PHE 168, LEU 328, TYR 326, PHE 343, MET 436, TYR 435, TYR 60	Pi-Pi Stack: TYR 435, TYR 398, TYR 326
Anthrone	-8.748	TYR 435	TYR 60, LEU 328, PHE 343, TYR 326, TYR 398, PHE 168, LEU 171, CYS 172, TYR 435, ILE 198, ILE 199	Pi-Pi Stack: PHE 343, TYR 326, TYR 398
Ferulic acid	-7.939	THR 201, TYR 326	LEU 328, TYR 326, PHE 99, PRO 102, PHE 103, PRO 104, ILE 316, LEU 88, ILE 199, CYS 172, LEU 171, PHE 168, LEU 167, LEU 164, TRP 119	None
Selegiline	-7.416	None	TRP 199, ILE 316, ILE 199, ILE 198, CYS 172, LEU 171, PHE 168, LEU 167, LEU 164, PRO 104, PHE 103, PRO 102, TYR 326, LEU 328, PHE 343	None
Rasagiline	-7.161	ILE 199	LEU 88, ILE 316, PRO 102, LEU 167, PHE 168, TRP 119, LEU 171, CYS 172, TYR 326, ILE 198, ILE 199, LEU 328	Pi-Pi Stack: TYR 326

Table 4ii: Hydrogen Bonds, Hydrophobic interactions, and other contacts of the ligands of *B. pinnatum* and the standard AChE inhibitors with AChE

Compound Name	Docking Score (kcal/mol)	H-BOND	Hydrophobic interacting amino acids	Other Interactions
Chrysin	-9.214	TYR 435	TYR 398, TYR 435, CYS 172, LEU 171, PHE 168, LEU 167, ILE 316, ILE 198, ILE 199, TRP 119, PHE 343, TYR 60, LEU 328, TYR 326	None
Pinoresinol	-10.281	ILE 199	TYR 398, CYS 172, LEU 171, ILE 198, ILE 199, PHE 168, LEU 328, TYR 326, PHE 343, MET 436, TYR 435, TYR 60	Pi-Pi Stack: TYR 435, TYR 398, TYR 326
Anthrone	-8.748	TYR 435	TYR 60, LEU 328, PHE 343, TYR 326, TYR 398, PHE 168, LEU 171, CYS 172, TYR 435, ILE 198, ILE 199	Pi-Pi Stack: PHE 343, TYR 326, TYR 398
Ferulic acid	-7.939	THR 201, TYR 326	LEU 328, TYR 326, PHE 99, PRO 102, PHE 103, PRO 104, ILE 316, LEU 88, ILE 199, CYS 172, LEU 171, PHE 168, LEU 167, LEU 164, TRP 119	None
Selegiline	-7.416	None	TRP 199, ILE 316, ILE 199, ILE 198, CYS 172, LEU 171, PHE 168, LEU 167, LEU 164, PRO 104, PHE 103, PRO 102, TYR 326, LEU 328, PHE 343	None
Rasagiline	-7.161	ILE 199	LEU 88, ILE 316, PRO 102, LEU 167, PHE 168, TRP 119, LEU 171, CYS 172, TYR 326, ILE 198, ILE 199, LEU 328	Pi-Pi Stack: TYR 326

The 2D-molecular interactions depicted in Figure 7 and 8 and the 3D-molecular interactions depicted in Figure 9 and 10 show that the selected ligands and standard drugs exhibit some common hydrogen bonds, pi-pi stacking, and hydrophobic interactions with the amino acid residues of MAO-B (4A7A) and AChE (7E3H) crystal structures. These interactions are essential for ligand-protein binding, complex stability, and specificity. The selected ligands, chosen for their BBB-crossing ability [29], demonstrate strong hydrophobic interactions with the target proteins, as shown in Table 4(i) and 4(ii). For example, ferulic acid exhibits more hydrophobic interactions with MAO-B (ID: 4A7A) than the standard drug rasagiline, while pinoresinol has more hydrophobic interactions with AChE (ID: 7E3H) than the standard drugs galantamine and rivastigmine. These findings suggest that the selected ligands could serve as potent antagonists of MAO-B and AChE in brain disorders, potentially surpassing the efficacy of standard drugs. Pi-pi stacking and hydrophobic interactions play crucial roles in protein folding, thermal stability, and ligand binding [30, 31].

Table 5i: In-silico drug-likeness predictions of the selected *B. pinnatum* ligands and the standard MAO-B inhibitors

Compound Name	Docking Score	H-BOND	Hydrophobic interacting amino acids	Other Interactions
Dracylic acid	-7.490	PHE 295, ARG 296	TYR 124, TYR 72, TYR 341, TRP 286, PHE 297, PHE 295, VAL 294, PHE 338	Pi-Pi Stack: TRP 286
Octanoic acid	-6.406	ARG 296, PHE 295	TYR 337, PHE 338, TYR 341, VAL 294, PHE 295, PHE 297, LEU 289, TRP 286, TYR 124	None
Niacin	-7.102	PHE 295, TYR 124	TYR 341, PHE 338, TYR 124, PHE 297, PHE 295, VAL 294, TRP 286	None

Pinoresinol	-10.767	TRP 86, ARG 296	TYR 72, TYR 124, TYR 133, TRP 86, ILE 451, TYR 337, PHE 338, TYR 341, VAL 294, PHE 295, PHE 297, LEU 289, TRP 286	None
Coumarin	-7.696	PHE 295	TYR 72, TRP 286, TYR 341, TYR 124, PHE 338, PHE 297, PHE, 295, VAL 294	Pi-Pi Stack: TRP 286
Donepezil	-11.186	PHE 295	TYR 72, LEU 289, TRP 286, TYR 341, TYR 124, PHE 338, TYR 337, TYR 133, ILE 451, TRP 86, PHE 297, PHE 295, VAL 294	Pi-Pi Stack: TRP 286, TRP 86
Galantamine	-7.002	None	TYP 124, TYR 72, TRP 286, LEU 289, PHE 338, TYR 341, PHE 297, PHE 295, VAL 294	Pi-Pi Stack: TRP 286
Rivastigmine	-6.104	None	TYR 124, TYR 337, PHE 338, TYR 341, TRP 286, PHE 297, PHE 295, VAL 294, TRP 86, TYR 124	Pi-Pi Stack: TYR 337, PHE 338

Table 5ii: In-silico drug-likeness predictions of the selected *B. pinnatum* ligands and the standard AChE inhibitors. (7E3H)

COMPOUNDS	MW	HBA	HBD	TPSA	ILOGP	LOGKP	ROV
Chrysin	254.24	4	2	70.67	2.27	-5.35	0
Pinoresinol	358.40	6	2	77.38	2.67	-6.87	0
Anthrone	194.23	1	0	17.07	2.21	-4.89	0
Ferulic acid	194.18	4	2	66.76	1.62	-6.41	0
Selegiline	187.28	1	0	3.24	2.80	-5.38	0
Rasagiline	171.24	1	1	12.03	2.51	-6.05	0

Table 5(i) and (ii) present the *in-silico* druglikeness predictions of *B. pinnatum* phyto-constituents and standard inhibitors with the target proteins. These predictions are based on the Lipinski Rule of Five (ROV), BBB, and toxicity study which evaluates the drug-like properties of a compound. ROV states that a compound should not exceed 500 Daltons in molecular weight (MW), have no more than 10 hydrogen bond acceptors (HBA) and 5 hydrogen bond donors (HBD), and have a LogP (partition coefficient) value not less than five. Adhering to these rules is crucial for a compound to be considered a drug [32, 33]. The selected compounds, including those from *B. pinnatum* and standard inhibitors, comply with all the Lipinski ROV criteria, indicating their potential as orally active drugs.

The absorption, distribution, metabolism, excretion, and toxicity properties of the selected *B. pinnatum* phytochemicals and standard inhibitors were assessed using admetSAR. Fig 11i displays a heat map of ADMET parameters, where yellow rectangles indicate positive or active compounds, and red rectangles indicate negative or inactive compounds. The heat map reveals that all the compounds, including those from *B. pinnatum*, can cross the BBB. Additionally, chrysin, pinoresinol, and ferulic acid exhibit high UGT catalysis, facilitating efficient metabolism and elimination of these compounds. Furthermore, chrysin, pinoresinol, and anthrone show positive results for thyroid receptor binding, which is important for modulating neuroinflammation and oxidative stress in neurodegenerative disorders. The study indicates that the selected compounds, including pinoresinol, are non-substrates for P-glycoprotein, allowing for greater bioavailability and efficacy.

Pinoresinol also acts as an inhibitor of P-glycoprotein, enhancing the effectiveness and bioavailability of co-administered drugs. Anthrone and ferulic acid exhibit high oral bioavailability, indicating a significant fraction reaching the systemic circulation after

oral administration. The compounds do not inhibit the human ether-go-go-related gene and can be absorbed by the human intestine. Chrysin and pinoresinol are not hepatotoxic and do not cause damage to the liver. Drug eye corrosion is the ability of a drug to cause damage to the eye and the surrounding tissues [34]. Chrysin, pinoresinol and anthrone have no eye damaging properties.

Cytochrome P450 is an enzyme that is involved in the metabolism of drugs and the most important isoforms of cytochrome P450 are CYP3A4, CYP2D6, CYP2C9, CYP2C19 and CYP1A2 [35]. Thus, inhibition of cytochrome P450 isoforms can affect the metabolism of drugs and increase the risk of toxicity. Furthermore, all the compounds display no carcinogenicity or mutagenic effects based on the ADMET test data.

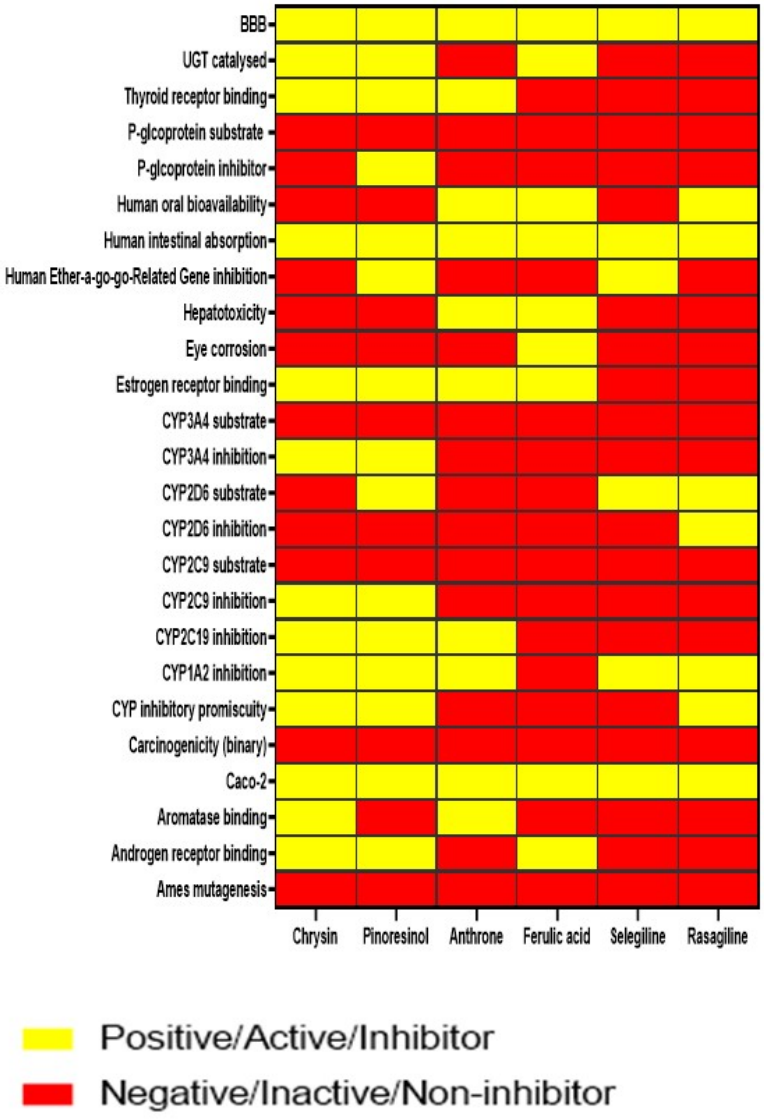

Figure 11i: A heat map illustration of the ADMET parameters of selected *B. pinnatum* phytochemicals and the standard MAO-B inhibitors (Selegiline and Rasagiline)

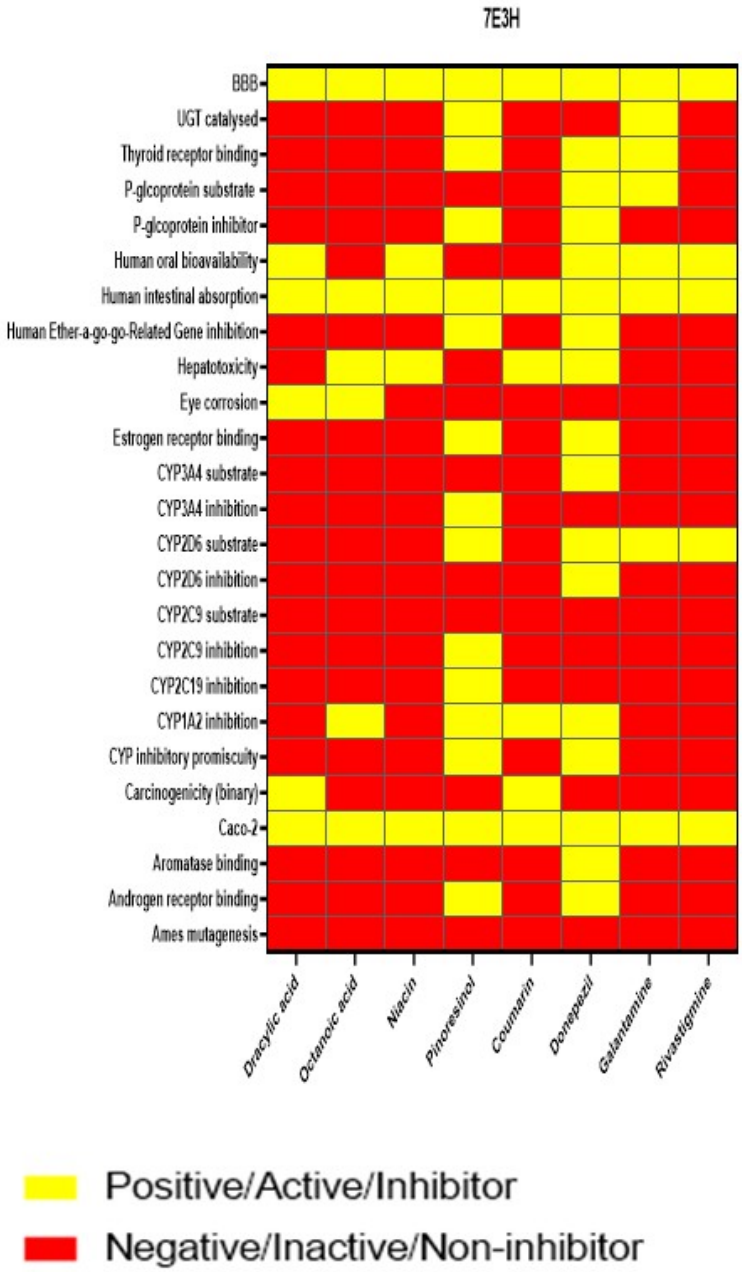

Figure 11ii: A heat map illustration of the ADMET parameters of selected *B. pinnatum* phytochemicals and the standard AChE inhibitors (Donepezil, Galantamine and Rivastigmine)

The heat map analysis (Fig 11ii) demonstrates that all selected compounds, including pinoresinol, can cross the BBB. Pinoresinol exhibits high catalysis by uridine glucuronyl transferase, aiding in the efficient metabolism and elimination of the compound. It also shows positive binding to thyroid receptors, which play a crucial role in neuroinflammation and oxidative stress modulation. Pinoresinol acts as an inhibitor of P-glycoprotein, enhancing the effectiveness and bioavailability of co-administered drugs by impeding their transport out of cells [36]. Dracylic acid and niacin have high oral bioavailability and are non-inhibitors of the human ether-go-go-related gene. All tested compounds can be absorbed by the human intestine. Dracylic acid and pinoresinol are non-hepatotoxic, posing no harm to the liver. Niacin, pinoresinol, and coumarin do not cause eye corrosion. The compounds do not exhibit inhibition of crucial cytochrome P450 isoforms, reducing the risk of drug metabolism interference. Octanoic acid, niacin, and pinoresinol do not show carcinogenicity effects. These compounds tested exhibit no mutagenic effects.

Overall, the test AChE inhibitors displayed significant inhibitory activity against AChE, suggesting its potential as a candidate for

enhancing cholinergic neurotransmission and addressing cognitive impairments associated with AD. The test MAO-B inhibitors on the other hand, demonstrated significant inhibitory activity against MAO-B, pronouncing their potential in maintaining dopamine levels and alleviating motor symptoms in PD. The identification of phytochemicals in *B. pinnatum* with inhibitory potential against AChE and MAO-B highlights its pharmacological relevance and validates its traditional medicinal uses. The binding free energies of these compounds to AChE and MAO-B were found to have a good correlation with other experimental inhibitory activities and the standard drugs.

Recommendation and Limitation of the study

This work primarily relies on *in silico* methods, which, while efficient and cost-effective, have limitations. *In silico* predictions may not fully capture the complex biological interactions and metabolic processes in living organisms. To enhance the robustness of the findings, future research should include *in vitro* assays to validate the binding affinity and inhibition efficiency of the identified blockers. Additionally, *in vivo* studies on appropriate animal models could be conducted to assess the pharmacokinetics, toxicity, and therapeutic potential, providing a more comprehensive evaluation of the candidate compounds.

Conclusion

This study explored *B. pinnatum* phyto-ligands as a source of natural inhibitors against AChE and MAO-B which are enzymes implicated in the pathophysiology of AD and PD, respectively. The phytochemical composition of *B. pinnatum* was structurally analyzed, and the inhibitory effects of its compounds on AChE and MAO-B were evaluated. The phytochemical analysis revealed the presence of various bio-active compounds, including flavonoids, alkaloids, phenolics, and terpenoids in *B. pinnatum*. These compounds possess diverse pharmacological activities and have shown potential in the management of neurodegenerative diseases. In this study, pinoresinol, octanoic acid, dracylic acid, naicin and coumarin; ferulic acid, chrysin, anthrone and pinoresinol showed to be excellent blockers of AChE and MAO-B, respectively, for the treatment of neurological disorders (AD and PD). The findings of this study contribute to the growing body of evidence supporting the use of natural products as sources of therapeutic agents for neurodegenerative disorders. Pinoresinol is strategically the best blocker of both enzymes in this study so it holds promise as lead molecules for further optimization and development of both therapeutics and treatment for AD and PD. However, *in silico* study is pivotal in drug development, it is also important to verify these findings using *in-vivo* and *in vitro* methods on the plant's ligand.

References

1. Maresova P, Hruska J, Klimova B, Barakovic S, Krejcar O (2020) Activities of daily living and associated costs in the most widespread neurodegenerative diseases: a systematic review. Clinical interventions in aging, 1841-62.

2. Balestrino R, Schapira AHV (2020) Parkinson disease. European journal of neurology, 27: 27-42.

3. Rajagopalan V, Venkataraman S, Rajendran DS, Kumar VV, Kumar VV et al. (2023) Acetylcholinesterase biosensors for electrochemical detection of neurotoxic pesticides and acetylcholine neurotransmitter: A literature review. Environmental Research, 115724.

4. Dvir H, Silman I, Harel M, Rosenberry TL, Sussman JL (2010) Acetylcholinesterase: from 3D structure to function. Chemico-biological interactions, 187: 10-22.

5. Akıncıoğlu H, Gülçin İ (2020) Potent acetylcholinesterase inhibitors: potential drugs for Alzheimer's disease. Mini reviews in medicinal chemistry, 20: 703-715.

6. Eldufani J, Blaise G (2019) The role of acetylcholinesterase inhibitors such as neostigmine and rivastigmine on chronic pain and cognitive function in aging: A review of recent clinical applications. Alzheimer's & Dementia: Translational Research & Clinical Interventions, 5: 175-183.

7. Manzoor S, Hoda N (2020) A comprehensive review of monoamine oxidase inhibitors as Anti-Alzheimer's disease agents: A review. European journal of medicinal chemistry, 206: 112787.

8. Prete BR, Ouanounou A (2021) Medical Management, Orofacial Findings, and Dental Care for the Patient with Parkinson's Disease. J Can Dent Assoc, 16.

9. Lieberman JA (2004) Dopamine Partial Agonists. CNS Drugs, 18: 251-67.

10. Fahn S (2008) The history of dopamine and levodopa in the treatment of Parkinson's disease. Movement disorders: official journal of the Movement Disorder Society, 23: S497-S508.

11. Ayano G (2016) Dopamine: Receptors, Functions, Synthesis, Pathways, Locations and Mental Disorders: Review of Literatures. J MentDisord Treat, 2: 120.

12. Mule P, Upadhye M, Taru P, Dhole S (2020) A Review on Bryophyllum pinnatum (Lam.) Oken. Research Journal of Pharmacognosy and Phytochemistry, 12: 111-3.

13. Yu W, MacKerell AD (2017) Computer-aided drug design methods. Antibiotics: methods and protocols, 85-106.

14. Murugan NA, Pandian CJ, Jeyakanthan J (2021) Computational investigation on Andrographis paniculata phytochemicals to evaluate their potency against SARS-CoV-2 in comparison to known antiviral compounds in drug trials. Journal of Biomolecular Structure and Dynamics, 39: 4415-26.

15. Ragoza M, Masuda T, Koes DR (2022) Generating 3D molecules conditional on receptor binding sites with deep generative models. Chemical science, 13: 2701-13.

16. Sahayarayan JJ, Rajan KS, Vidhyavathi R, Nachiappan M, Prabhu D et al. (2021) In-silico protein-ligand docking studies against the estrogen protein of breast cancer using pharmacophore based virtual screening approaches. Saudi Journal of Biological

Sciences, 28: 400-7.

17. SwissADME (http://www.swissadme.ch) online server, Pro-Tox II (https:// tox-new.charite.de/protox II) online server and ADMETsar (https://Immd.ecust.edu.cn) online servers.

18. Pratama MRF, Poerwono H, Siswodiharjo S (2019) ADMET properties of novel 5-O-benzoylpinostrobin derivatives. Journal of Basic and Clinical Physiology and Pharmacology, 30.

19. Ma'ruf NQ, Hotmian E, Tania AD, Antasionasti I, Fatimawali F et al. (2022) In silico analysis of the interactions of Clitoria ternatea (L.) bioactive compounds against multiple immunomodulatory receptors. In AIP Conference Proceedings, 2638: 1.

20. Pang J, Gao S, Sun Z, Yang G (2021) Discovery of small molecule PLpro inhibitor against COVID-19 using structure-based virtual screening, molecular dynamics simulation, and molecular mechanics/Generalized Born surface area (MM/GBSA) calculation. Structural Chemistry, 32: 879-86.

21. Aarsland D, Batzu L, Halliday GM, Geurtsen GJ, Ballard C et al. (2021) Parkinson disease-associated cognitive impairment. Nature Reviews Disease Primers, 7: 47.

22. Alrouji M, Al-Kuraishy HM, Al-Gareeb AI, Zaafar D, Batiha GES (2023) Orexin pathway in Parkinson's disease: a review. Molecular Biology Reports, 1-14.

23. Marucci G, Buccioni M, Dal Ben D, Lambertucci C, Volpini R et al. (2021) Efficacy of acetylcholinesterase inhibitors in Alzheimer's disease. Neuropharmacology, 190: 108352.

24. Marotta G, Basagni F, Rosini M, Minarini A (2020) Memantine derivatives as multitarget agents in Alzheimer's disease. Molecules, 25: 4005.

25. Rastelli G, Rio AD, Degliesposti G, Sgobba M (2010) Fast and accurate predictions of binding free energies using MM-PBSA and MM-GBSA. Journal of computational chemistry, 31: 797-810.

26. Mease P (2005) Fibromyalgia syndrome: review of clinical presentation, pathogenesis, outcome measures, and treatment. The Journal of Rheumatology Supplement, 75: 6-21.

27. Schaller D, Šribar D, Noonan T, Deng L, Nguyen TN et al. (2020) Next generation 3D pharmacophore modeling. Wiley Interdisciplinary Reviews: Computational Molecular Science, 10: e1468

28. Joshi T, Joshi T, Sharma P, Mathpal S, Pundir H et al. (2020) In silico screening of natural compounds against COVID-19 by targeting Mpro and ACE2 using molecular docking. Eur Rev Med Pharmacol Sci, 24: 4529-36.

29. Istifli ES, Netz PA, Sihoglu Tepe A, Husunet MT, Sarikurkcu C et al. (2022) In silico analysis of the interactions of certain flavonoids with the receptor-binding domain of 2019 novel coronavirus and cellular proteases and their pharmacokinetic properties. Journal of Biomolecular Structure and Dynamics, 40: 2460-74.

30. Vernon RM, Chong PA, Tsang B, Kim TH, Bah A et al. (2018) Pi-Pi contacts are an overlooked protein feature relevant to phase separation. elife, 7: e31486.

31. Chen T, Li M, Liu J (2018) π–π stacking interaction: a nondestructive and facile means in material engineering for bioapplications. Crystal Growth & Design, 18: 2765-83.

32. Olugbogi EA, Bodun DS, Omoseeye SD, Onoriode AO, Oluwamoroti FO et al. (2022) Quassia amara bioactive compounds as a Novel DPP-IV inhibitor: an in-silico study. Bulletin of the National Research Centre, 46: 1-14.

33. Ma'ruf NQ, Hotmian E, Tania AD, Antasionasti I, Fatimawali F et al. (2022) In silico analysis of the interactions of Clitoria ternatea (L.) bioactive compounds against multiple immunomodulatory receptors. In AIP Conference Proceedings, 2638: 1.

34. Wang R, Gao Y, Liu A, Zhai G (2021) A review of nanocarrier-mediated drug delivery systems for posterior segment eye disease: Challenges analysis and recent advances. Journal of Drug Targeting, 29: 687-702.

35. Ogidigo JO, Anosike C, Nwodo OFC, Omotuyi O, Nash O et al. (2018) In silico molecular docking and pharmacokinetic studies of some selected phyto-constituents of Byrophyllum pinnatum as a potential selective inhibitor of MAO-B. Pharmacology-online, 3: 14-49.

36. González ML, Vera DM A, Laiolo J, Joray MB, Maccioni M et al. (2017) Mechanism underlying the reversal of drug resistance in P-glycoprotein-expressing leukemia cells by pinoresinol and the study of a derivative. Frontiers in pharmacology, 8: 205.